IEEE Access
Multidisciplinary | Rapid Review | Open Access Journal

Received March 12, 2022, accepted March 29, 2022, date of publication April 4, 2022, date of current version April 8, 2022.

Digital Object Identifier 10.1109/ACCESS.2022.3164422

PE-A* Algorithm for Ship Route Planning Based on Field Theory

YIHUA LIU[1], TING WANG[1], AND HONGZHI XU[2]
[1]Merchant Marine College, Shanghai Maritime University, Shanghai 200000, China
[2]Shandong Shipping Corporation, Qingdao 266000, China

Corresponding author: Yihua Liu (liuyh@shmtu.edu.cn)

This work was supported in part by the National Natural Science Foundation of China under Grant 51509151, in part by the Shandong Province Key Research and Development Project under Grant 2019JZZY020713, in part by the Shanghai Commission of Science and Technology Project under Grant 21DZ1201004, and in part by the Anhui Provincial Department of Transportation Project under Grant 2021-KJQD-011.

ABSTRACT Route planning is the key to safe, efficient and intelligent navigation of maritime traffic. Autonomous route planning is a complex optimization problem, which requires both global route planning and local collision avoidance. In this paper, we propose an optimization algorithm which can consider both global route planning and local collision avoidance. Firstly, nonlinear constraint optimization models of obstacle limitation, safe water depth limitation and ship steering limitation are established. Then, the PE-A* algorithm and route planning framework are proposed by using potential energy field to accurately express the environment. Finally, the safety and feasibility of the route planned by PE-A* algorithm are discussed through simulation experiments. Simulation results show that PE-A* algorithm can realize both global route planning and local collision avoidance, and the safety and feasibility of the planned route are greatly improved. From the perspective of potential energy, this work proposes an automatic route planning algorithm and establishes a flexible mathematical model, which can add fuel consumption, time and other related engineering requirements into the model to plan the optimal route meeting the requirements.

INDEX TERMS Ship, potential energy, A* algorithm, route planning.

I. INTRODUCTION

With the development of intelligent transportation industry, sea, land and air are developing to the direction of autonomous driving, its four cores: positioning, perception, planning and decision-making, path planning has been one of the key issues of autonomous driving. According to the starting point, destination and known environmental information, we shall perceive the dynamic environmental information around, plan the initial path and navigation decisions. According to the motion characteristics of different vehicles, road traffic belongs to two dimensions, aviation belongs to three dimensions, and water traffic is between them. Ship route planning must consider ship maneuvering restrictions, complex marine environment, and traffic related dynamic information. Excellent route planning algorithms need to take into account both global route planning and local dynamic obstacle avoidance, so as to achieve the true sense of automatic ship route planning.

The associate editor coordinating the review of this manuscript and approving it for publication was Zhenzhou Tang.

Automatic ship route planning needs to solve two major problems [1]: (1) global route planning: route planning is carried out in a known static environment. (2) Local dynamic collision avoidance: it is necessary to collect the information of the surrounding dynamic environment in real time through sensors, obtain the position of the current position map and the distribution of local obstacles for local dynamic collision avoidance. The ship navigates in the global planned route and avoids local obstacles when encountering new dynamic obstacles. Instead, follow the planned route.

A. GLOBAL ROUTE PLANNING

In the aspect of global route planning, many researchers have studied from different angles and achieved good results. At present, ships are installed with AIS equipment, a large amount of AIS data contains historical navigation information, Zhang *et al.*. An automatic path design method based on Simple Round Unit (SRU) and Automatic Identification System (AIS) data is proposed. The relationship between ship routes is extracted using AIS tracking data to generate ship routes and speed [2]. However, this method relies on

the quantity and quality of AIS data, it is difficult to obtain the optimal route for areas with less AIS data or poor AIS data quality. Machine learning algorithm can train better experimental data sets to improve the accuracy of ship fuel consumption prediction. Some scholars have applied it to global route planning, Bui-Duy *et al.*. Based on the deep machine learning method to estimate the fuel consumption model of the shipping line, the hybrid machine learning technology is constructed to predict the fuel consumption of ships and plan the optimal route that meets the expectation of minimizing the fuel cost of shipping companies [3]. Wen *et al.*. DBSCAN algorithm was used to identify key areas, these areas were automatically connected through clustering similarity measurement. Artificial neural network learned the relationship between turning areas under different ship sizes and planned reasonable routes [4].

Shipping companies need to consider many factors in global route planning, such as fuel consumption, safety, route length, route time and so on. A new evolutionary multi-objective optimization method based on tradeoff was proposed by Szlapczynska *et al.*, which used configurable weight interval to assign to all targets. Under the premise of taking dynamic weather conditions into consideration, the optimal route is designed in terms of time, fuel consumption, crew and cargo safety [5]. Chuang *et al.*. Proposed a fuzzy genetic algorithm suitable for liner transportation planning, which could not only consider the market demand, shipping and berthing time of container ships at the same time, but also find the most appropriate container ship route [6]. However, the calculation result depends on the value of weight, and it is always a difficult problem to select the right weight.

Many route planning algorithms have better results in some aspects, but also have shortcomings. For example, ant colony algorithm has strong robustness, but may fall into local optimal solution. Genetic algorithm has fast random search ability and good robustness, but the calculation results are dependent on the selection of initial population. A* algorithm is a heuristic search algorithm, which can get results quickly, but it depends on the construction of the environmental accuracy. When the environmental accuracy is poor, the planned route is often not feasible. Some scholars improved the above algorithm and the improved algorithm obtained better results. Liang *et al.*. Proposed the leader-Vertex Ant Colony Optimization (LVACO) algorithm, which ensures the leader of the ant colony and uses the vertex method to optimize the path. The path planned by LVACO has fewer unnecessary path points and is more suitable for navigation [7]. Lan *et al.*. Proposed an improved path planning algorithm integrating A-Star algorithm and ant colony algorithm, which solved the problems of slow convergence, large number of iterations and long search time of ant colony algorithm in robot global path planning and the problem that ant colony algorithm is easy to fall into local optimization in complex environment [8]. Li *et al.*. Proposed a multi-direction A* algorithm to reduce the number of search nodes, further shorten the search path, and make AUV 3D path planning efficient and real-time [9]. Han *et al.*. introduced a meta-heuristic Whale Optimization Algorithm (WOA), which can help ships find safe routes with low energy consumption in large and complex ocean environments [10].

Planning the optimal route requires the formation of an accurate environment. Raster map storage environment has a small space occupancy rate, but the accuracy of environment description is poor. Wang *et al.*. Proposed a global path planning framework based on hybrid mapping. Calculate the global path from the scene diagram, map the path to the lower level and generate the geometric path. Since the high level is generated by the low level, the global path can provide strong guidance for the calculation of measurement paths [11]. Xie *et al.*. Proposed a 2.5D navigation graph method for modeling the walking domain and an improved A* algorithm for path planning of large ships in 3D virtual environment, which can better solve the problem of path planning of ships in 3D VE [12].

As can be seen from the above research results, some scholars have achieved good research results on global route planning from different perspectives, such as mining navigation information through AIS data, optimizing route planning algorithms, and constructing mathematical models for optimal route planning.

B. LOCAL DYNAMIC COLLISION AVOIDANCE

The cause of ship collision is that the distance between ships and obstacles is too close. Ship collision avoidance can be achieved by changing course and changing speed. Zhang *et al.*. proposed the idea of changing speed to avoid collision, which not only avoids blind obedience to COLREGS rules, but also reduces deviation from planned route [13]. Liu *et al.*. The collision avoidance trajectory of ships based on models is closer to the target ship than that without models, and the DCPA value is significantly smaller after models are added. The research results are in line with the minimum DCPA and TCPA of the actual situation to ensure that the ship takes avoidance measures in advance [14].

Local collision avoidance is a micro level operation, which requires high precision of environment construction. Xie *et al.*. Proposed A multi-direction A* algorithm, which iteratively searched for the optimal neighbor nodes, avoided the merger between adjacent obstacles, improved the resolution of the grid, and greatly improved the efficiency of local route planning. This algorithm avoids the disadvantage that rasterization of environment leads to the reduction of feasible water area, but it does not consider whether ships can navigate safely in narrow space [15]. Based on the dynamic path planning model proposed by Li *et al.*. ABC algorithm is applied to the path optimization of invading submarine. This method is a feasible approach to submarine search evasive path planning. However, this algorithm considers local collision avoidance in 2D environment without considering the draft requirements of actual ships, so it is difficult to apply this algorithm to autonomous collision avoidance of

ships [16]. Su *et al.*. Studied a collision avoidance method which takes into account the steering difficulty and large inertia of large ships. Considering ship maneuverability, the ship risk model is established and collision avoidance decision is given according to COLREGS. This method is suitable for large ships in development waters and has high accuracy and reliability [17].

Local collision avoidance needs to be judged quickly and has high requirements on the calculation speed of the algorithm. Some scholars have improved the algorithm so that it can get the local collision avoidance path quickly. Liu *et al.*. Combined the improved bacterial foraging algorithm with the particle swarm optimization algorithm with strong global search ability and fast local convergence ability and applied it to ship collision avoidance path optimization. The hybrid optimization algorithm could get collision avoidance path quickly [18]. By modeling the dynamic domain of ships, a reasonable and effective ship automatic collision avoidance decision system was established by Xu *et al.*. Collision was simulated to evaluate the performance of the proposed formula [19].

Before the local collision avoidance operation, the ship should be able to obtain the collision avoidance decision quickly, and return to the global route with a good attitude after the operation. Yu *et al.*. Proposed a fast decision- making method for ship collision avoidance diversion. In order to reduce the number of calculation targets, a clustering analysis method is introduced, the voyage loss is taken as the objective function and a deterministic optimization algorithm is adopted to quickly obtain the optimal collision avoidance rerouting decision in the global scope. This method enables ships to quickly avoid local obstacles and greatly reduces the risk of ship collision [20]. Shi *et al.*. Used the recovery path planning algorithm based on Dubins Curve. The recovery path given by the algorithm can make the AUV navigate underwater along the smooth curvature trajectory and safely enter the recovery platform from the specified position with the desired attitude [21].

Many scholars also made great contributions to ship collision avoidance system, Jincan *et al.*. Collision avoidance warning system for ships based on ECDIS and AIS [22]. Chen *et al.*. Proposed an artificial position field method suitable for unmanned ships. Its main contributions include potential field analysis and collision avoidance controller design in an environment with obstacles [23]. Namgung *et al*. Proposed a MASS collision risk reasoning system that conforms to COLREGS key rules for collision avoidance. The system takes into account all important variables in collision avoidance guidelines that comply with COLREGs rules, thus improving the timing and location of potential collision warnings. Thus, providing more decision-making time for taking necessary anti-collision measures [24]. Wang *et al.*. Proposed a new collision avoidance decision system for autonomous ships. According to the latest information, the system outputs collision avoidance decision at a certain frequency, which is suitable for practical ship application. Front end and back end are two main components of the system. The front end provides preliminary information and the back end generates collision avoidance decisions. Robustness and effectiveness of the collision avoidance decision system in various marine scenarios [25].

C. TAKE INTO ACCOUNT DYNAMIC AND STATIC PLANNING

At present, only a few algorithms can realize global route planning and local dynamic collision avoidance at the same time. To realize truly autonomous route planning and further promote the automatic navigation of ships, route planning algorithm must consider both global planning and local collision avoidance. Zhang *et al.*. Proposed a dynamic path planning method for underwater unmanned vehicle (UUV) in global uncertain environment based on sonar detection data. This method is time-consuming for dynamic planning, and can well meet the real-time requirements in complex and unknown dynamic environment [26]. Tian *et al.*. Proposed an incremental PID algorithm for ship automatic heading control. It allows the ship to avoid collisions with moving and static targets. Studies show that the multi-ship collision avoidance concept based on speed obstacle is effective and can provide support for the automatic collision avoidance system of ships [27]. Wang *et al.*. proposed the ultimate optimization of A* (FO a*) algorithm for USV automatic route planning, and designed a nonlinear tracking controller to ensure ship navigation on the route. The algorithm and nonlinear tracking controller are effective and deterministic for offline path planning [28]. Wang *et al.*. proposed a quadratic optimization genetic algorithm based on ship motion characteristics. Considering the constraints of ship maneuvering characteristics, an efficient and feasible dynamic ship route planning solution is realized for the complex problem of integrated collision avoidance planning under static and dynamic obstacles [29]. All the above algorithms can avoid dynamic and static obstacles well, but are mainly carried out from the Angle of collision avoidance, lacking the route planning from the macro-Angle. From the global point of view, the routes planned by the above algorithms are not optimal, and most algorithms still choose different algorithms in global planning and local collision avoidance, without realizing the unification of algorithms.

According to the literature review, autonomous route planning can be regarded as an optimization problem. There are still some problems that need to be improved:

(1) traditional airline planning cannot give consideration to both global airline planning and local dynamic collision avoidance, so autonomous airline planning in a real sense cannot be achieved.
(2) Route planning has high requirements on environmental description. Global route planning has a large environmental description range and low accuracy requirements, while local dynamic obstacle avoidance has a small environmental description range and high accuracy

requirements. It is one of the difficulties to describe the global and local environment reasonably, which directly affects the feasibility of the planned route.

(3) The conventional mathematical model of route planning considers few limiting factors, so it is necessary to establish a flexible model to meet different needs.

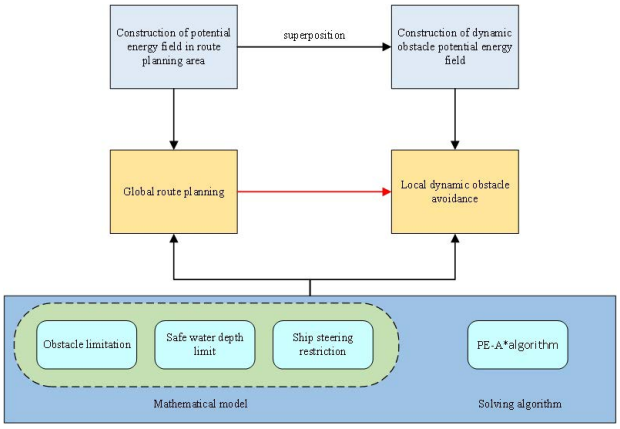

FIGURE 1. The structure of the present paper.

The structure of the paper is shown in Fig. 1. The PE-A* algorithm is proposed in this paper to realize the independent planning of ship routes. Firstly, the mathematical description of route planning is carried out, and the mathematical model of route planning is established considering obstacle restriction, safe water depth restriction and ship turning restriction. Secondly, potential energy field is used to describe ship route environment. Finally, A PE-A* algorithm is proposed which takes into account both global route planning and local dynamic obstacle avoidance. From the perspective of the theory, the whole process of navigation of ships, with traction potential energy field and safety potential energy field covers navigation area, the environment on the influence of the navigation of ships is converted to potential energy field of the ship, the influence of safety potential value as A scalar superposition, it guarantees the dynamic description of navigation environment, makes the PE - A * algorithm to two or more things global route planning and local dynamic collision avoidance.

This paper is organized as follows. The second section describes the ship route mathematically. In the third section, the concept of field theory is introduced in detail, the potential energy field and collision potential energy definition in the water area of route planning are established. In the fourth section, a mathematical model of route planning considering obstacle restriction, safe water depth restriction and ship turning restriction is established. The fifth section, introduces PE-A* algorithm and route planning in detail. The sixth section, the route generation process is described in detail through experiments to verify the safety and feasibility of the route planned by PE-A* algorithm. The seventh section is the summary of the whole paper.

II. MATH GEOMETRIC DESCRIPITION OF SHIP ROUTE

The ship route is a directional, collision-free path that connects the origin and destination. From the perspective of geometry and mathematics, a line segment is the cumulative representation of a series of points in space. Similarly, the route is presented by the accumulation of time and space of every position that a ship passes through during its voyage. Because there are too many ship position points on the route, the position points requiring ship turning operation are selected as path planning nodes. The mathematical expression is as follows:

$$\begin{cases} P = \{P_1, P_2, \cdots P_i \cdots P_N\} \\ P_i = (x_i, y_i) \\ i \in [1, N] \end{cases} \tag{1}$$

P path point set, P_i is the i path point, where P_1 is the origin and P_N is the destination.

$$\begin{cases} L = \left\{ \underset{l_1}{\longrightarrow}, \underset{l_2}{\longrightarrow}, \cdots \underset{l_i}{\longrightarrow} \cdots \underset{l_{N-1}}{\longrightarrow} \right\} \\ \underset{l_i}{\longrightarrow} = \underset{P_iP_{i+1}}{\longrightarrow} = (x_{i+1} - x_i, y_{i+1} - y_i) \end{cases} \tag{2}$$

L represents section road set, $\underset{l_i}{\longrightarrow}$ represents section road i.

$$\begin{cases} E = \{ \underset{e_1}{\longrightarrow}, \underset{e_2}{\longrightarrow}, \cdots \underset{e_i}{\longrightarrow} \cdots \underset{e_{N-1}}{\longrightarrow} \} \\ \underset{e_i}{\longrightarrow} = \dfrac{\overrightarrow{l_i}}{|\underset{l_i}{\longrightarrow}|} = \dfrac{\overrightarrow{P_iP_{i+1}}}{|\underset{P_iP_{i+1}}{\longrightarrow}|} = \dfrac{(x_{i+1} - x_i, y_{i+1} - y_i)}{\sqrt{(x_{i+1} - x_i)^2 + (y_{i+1} - y_i)^2}} \end{cases} \tag{3}$$

E is the section direction set, $\underset{e_i}{\longrightarrow}$ is the navigation direction of section i.

$$\begin{cases} \theta_{i(i+1)} = \cos^{-1} < \underset{e_i}{\longrightarrow}, \underset{e_{i+1}}{\longrightarrow} > = \dfrac{\underset{e_i}{\longrightarrow} \cdot \underset{e_{i+1}}{\longrightarrow}}{\left|\underset{e_i}{\longrightarrow}\right| \cdot \left|\underset{e_{i+1}}{\longrightarrow}\right|} = \\ \dfrac{x_{i+1}x_i + y_{i+1}y_i}{\sqrt{(x_{i+1} - x_i)^2} \cdot \sqrt{(y_{i+1} - y_i)^2}} \\ \theta = \{\theta_{12}, \theta_{23}, \cdots \theta_{i(i+1)} \cdots \theta_{(N-1)N}\} \end{cases} \tag{4}$$

θ is the set of turning angle of ship route, $\theta_{i(i+1)}$ is the turning of i section and $i + 1$ section.

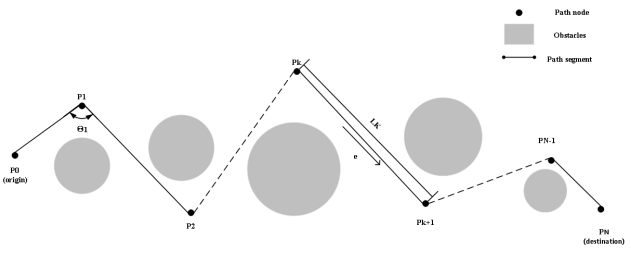

FIGURE 2. Diagram of ship route explanation.

As shown in Fig. 2, there are obstacles between the origin p_0 and the destination p_N that the ship cannot reach directly. The gray part is obstacle and the planned path is shown in Fig. 2. θ_1 is the first turning Angle of the planned route, L_k

is the k road section, $\underset{e_k}{\longrightarrow}$ is the navigation direction of the K section.

III. FIELD THEORY

In road traffic, Ni. D uses field theory to describe the vehicle driving environment, and has obtained some research results. Microscopic traffic flow model based on potential energy field theory can well represent the driving risks faced by vehicles in the process of driving [29]–[31]. Similarly, this theory can accurately describe the shipping route planning waters from the macro and micro perspectives.

The field theory is used to analyze the whole sailing process of a ship: the essence of a ship sailing on the sea is that the time and space state of the ship's position changes, the ship's position changes at different times and the environmental state of the same position changes at different times.

(1) Macro Angle: the ship is always sailing towards the destination, so there is a traction potential field between the destination and the ship, which constantly pulls the ship to the destination and avoids aimless sailing on the water surface.

(2) Microscopic Angle: Collision with obstacles bring great losses, so obstacles need to be avoided during navigation. Therefore, there is a safety potential energy field between ships and obstacles, which guides ships to go to safe areas to avoid obstacles.

A. TRACTION OTENTIAL FIELD

There is a traction potential energy field between the origin and the destination, so the ship is always affected by the traction potential energy field before arriving at the destination. The zero potential energy point of the traction potential energy field is the destination $E_f\ (destination) = 0$ and the traction potential energy value of the origin is $E_f(origin) = 1$. The traction potential energy value of different points is different. When the ship does not arrive at the destination, there is a traction potential difference between the ship position and the destination, the ship will move. On the contrary, the ship will not move.

The traction potential energy function at any point P is as follows:

$$E_f\ (x_P, y_P) = \frac{\sqrt{(x_P - x_{destination})^2 + (y_P - y_{destination})^2}}{\sqrt{(x_{origin} - x_{destination})^2 + (y_{origin} - y_{destination})^2}} \tag{5}$$

The potential energy difference function of any two points p_1 and p_2 is as follows:

$$\Delta E_f\ (p_1, p_2) = E_f\ (x_{P1}, y_{P1}) - E_f\ (x_{P2}, y_{P2}) \tag{6}$$

Potential energy difference direction from high potential energy point to low potential energy point:

$$\overrightarrow{\Delta E_f(P1,P2)} = \frac{(x_{i+1} - x_i, y_{i+1} - y_i)}{\sqrt{(x_{i+1} - x_i)^2 + (y_{i+1} - y_i)^2}} \tag{7}$$

TABLE 1. Traction potential field.

point	Potential energy value	Potential energy difference
A (origin)	$E_f(x_{P2}, y_{P2})$=1	$\lvert\overrightarrow{\Delta E_f(P_1,B)}\rvert = \lvert\overrightarrow{\Delta E_f(P_2,B)}\rvert$
P_1	$E_f(x_{P1}, y_{P1}) = \frac{\sqrt{(x_{P1} - x_B)^2 + (y_{P1} - y_B)^2}}{\sqrt{(x_A - x_B)^2 + (y_A - y_B)^2}}$	$\overrightarrow{\Delta E_f(P_1,B)} \neq \overrightarrow{\Delta E_f(P_2,B)}$ $\lvert\overrightarrow{\Delta E_f(P_2,A)}\rvert \neq \lvert\overrightarrow{\Delta E_f(P_2,B)}\rvert$ $\overrightarrow{\Delta E_f(P_2,A)} = \overrightarrow{\Delta E_f(P_2,B)}$
P_2	$E_f(x_{P2}, y_{P2}) = \frac{\sqrt{(x_{P2} - x_B)^2 + (y_{P2} - y_B)^2}}{\sqrt{(x_A - x_B)^2 + (y_A - y_B)^2}}$	
B (destination)	$E_f(x_B, y_B)$ =0	

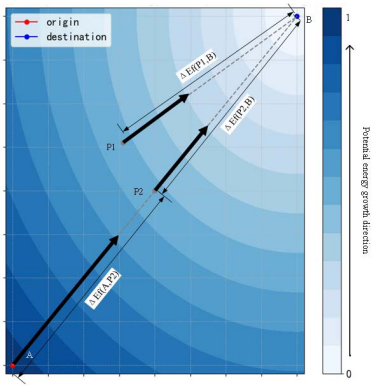

FIGURE 3. Diagram of traction potential energy field interpretation.

As shown in Fig. 3, A is the origin and B is the destination, p_1 and p_2 are the position points of navigation waters between two points. The traction potential energy values at point A, B, p_1 and p_2 are shown in Table 1: The traction potential energy value at point A is 1, and the potential energy value at point B is 0. The potential energy difference between points p_1 and B and between points p_2 and B is equal with different directions. The potential energy difference between A and p_2 and between p_2 and B is different but in the same direction.

B. SAFE POTENTIAL IELD

Obstacles affect the navigation of ships, so ships need to avoid obstacles to ensure navigation safety. The safe potential energy field of ship is established by field theory, and the influence of obstacles on ship navigation is reflected by the safe potential energy field. The influence of different positions of obstacles on the safety of ship navigation is directly reflected in different safety potential energy values. The function model is:

$$E_0\ (x, y) = \frac{b}{2\pi\sigma_{xt}\sigma_{yt}} e^{-\frac{(x-x_t)^2}{2\sigma_{xt}^2} - \frac{(y-y_t)^2}{2\sigma_{yt}^2}} \tag{8}$$

where $E_0\ (x, y)$ represents the safety potential energy value of point (x, y), the position of the center point of the obstacle at t time of (x_t, y_t), $E_o\ (x_t, y_t)$ is the safety potential energy value of the center point of the obstacle at t time, σ_{xt} and σ_{yt} represent the X-axis and Y-axis influence radius of the obstacle in the horizontal plane region at time t, and b is the

parameter adjustment coefficient between the function value and the actual elevation data of the obstacle.

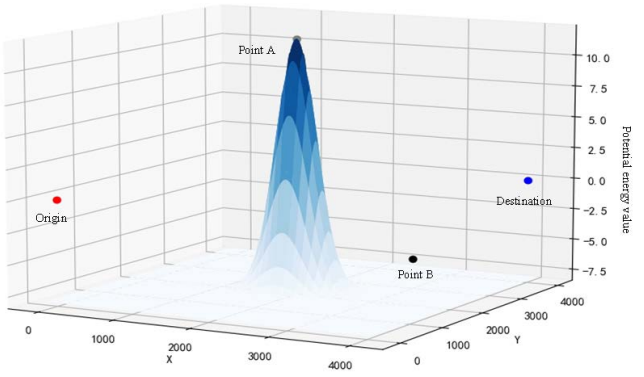

FIGURE 4. Schematic diagram of safe potential energy field interpretation.

The safe potential energy model of a single obstacle is shown in Fig. 4, the horizontal plane is the zero safe potential energy surface, point A is the center point of the obstacle, $E_0(x_a, y_a) > E_0(x_b, y_b)$. The single obstacle safety potential energy field is superimposed to obtain the safety potential energy field of sailing waters.

C. POTENTIAL NERGY DEFINITION OF COLLISION

The essence of ship collision is that the distance between ship and obstacle is less than the safe distance. From the point of view of field theory, the other ship is an obstacle to our ship, in the same way our ship is an obstacle to the other ship, so there are safety potential energy fields of both our ship and other ship. The potential energy field is changing as my ship moves with it. The minimum potential energy of the cross section α between the center point of the safety potential energy field of our ship $p_{o1} = (x_{o1}, y_{o1})$ and the center point of the safety potential energy field of other ship $p_{o2} = (x_{o2}, y_{o2})$ is $E_\alpha(x_{min}, y_{min})$. When the minimum potential energy is less than the safety potential energy threshold, collision occurs. Otherwise, there is no collision. The safe potential energy threshold is determined according to the ship's draft and other relevant information. The collision function model is:

$$\begin{cases} p_{o1} = (x_{o1}, y_{o1}) \\ p_{o2} = (x_{o2}, y_{o2}) \\ E_\alpha(x_{min}, y_{min}) > E_{safe} \end{cases} \tag{9}$$

$E_\alpha(x_{min}, y_{min})$ is the minimum safe potential energy value of potential energy field section α, E_{safe} represents the safe potential energy threshold.

As shown in Fig. 5 and Fig. 6, ships A, B and C have the same specifications, and ship D is smaller than ships A, B and C. When A ship is the main body, the other three ships are obstacles. Take the horizontal plane as the zero potential energy surface $E_{water} = 0$, safety threshold $E_{safe} = -8$, establish the safe potential energy field of the ship A, B, C, D. By the safety potential energy equipotential graph can

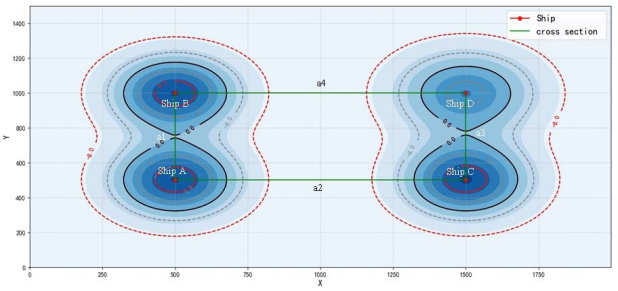

FIGURE 5. Schematic diagram of potential energy definition of collision.

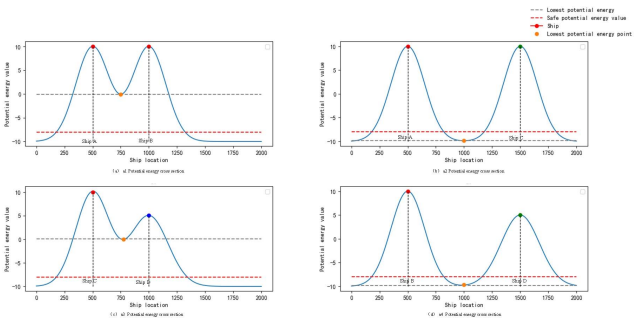

FIGURE 6. Section diagram of collision potential energy field.

be concluded that the ship A, B, C, D relative location and the distribution of the potential energy, the parts in red solid line is zero potential energy surface, red dashed part safe potential energy threshold line. It can be obtained from the safety equipotential line diagram and potential energy section diagram:

(1) Collison: It can be obtained from Fig. 6 that $minE_{a1}(x_{min}, y_{min}) > E_{safe}$ can be obtained from the potential energy section A1 between ship A and ship B. It can be seen that the safety equipotential line, lines of ship A and ship B blend. $minE_{a3}(x_{min}, y_{min}) > E_{safe}$ can be obtained from the potential energy section a3 between ships C and D. Combined with the Fig. 5, it can be seen that the safety equipotential line, lines of ships C and D are fused. Ships A and B are in the same type ship collision state, while ships C and D are in different type ship collision state.

(2) No Collision: It can be obtained from Fig. 6 that $minE_{a2}(x_{min}, y_{min}) > E_{safe}$ can be obtained from the potential energy section a2 between ships A and C. It can be seen that the safety Equipotential line, lines of ships A and C do not intersect. $minE_{a4}(x_{min}, y_{min}) > E_{safe}$ can be obtained from the potential energy section a4 between ships B and D. Combined with the Fig. 5, it can be seen that the safety equipotential line, lines of ships B and D do not intersect. Ships A and C are in the same type of ship without collision, and ships B and D are in different type of ship without collision.

IV. MATHEMATICAL MODEL

A. OBSTRUCTION RESTRICTION

Collisions are costly, Ships must steer clear of obstacles. When the safety potential energy value of the ship's position

is lower than the safety potential energy threshold, there is no collision. On the contrary, there is collision. The model is:

$$\boldsymbol{E_\alpha}\left(\boldsymbol{x_{min}}, \boldsymbol{y_{min}}\right) < \mathbf{E}_{\boldsymbol{safe}} \tag{10}$$

$E_{\boldsymbol{\alpha}}\left(x_{min}, y_{min}\right)$ is the minimum safe potential energy value of the section α of the safe potential energy field, E_{safe} represents the threshold of the ship's safe potential energy.

B. WATER DEPTH LIMIT

The relationship between the navigational water depth and the ship's safe water depth requirements for ships should be considered. When the navigational water depth is greater than the safe water depth requirements, the vessel may navigate in such waters. On the contrary, the ship cannot navigate in the waters. The model is:

$$H\left(x, y\right) \geq D \tag{11}$$

$H\left(x, y\right)$ represents the water depth of navigational waters, D represents safe water depth requirements for ships.

C. STEERING ANGLE CONSTRAINT

Due to the mechanical limitations of the ship itself, it is impossible to make emergency turning, the ship has the maximum turning constraint θ_{max}. The turning should be considered in route planning, which is also directly reflected in the turning Angle of the path node. The model is:

$$\theta_i < \theta_{max} \tag{12}$$

θ_i refers to the steering of the i-th route, and θ_{max} refers to the maximum steering constraint of the ship.

D. THE OBJECTIVE FUNCTION

In the traction potential energy field, the ship keeps sailing towards the destination (zero potential energy point). In the safety potential energy field, ships always sail at the position with a small safety potential energy value in order to avoid danger. In summary, under the joint influence of the traction potential energy field and the safety potential energy field, ships find the collision-free path to reach the end point, namely the path of the minimum safety potential energy. The objective function is:

$$minE_o\left(P_i\right) \tag{13}$$

To sum up, the route planning model are shown in the Table 2:

TABLE 2. Summary table of mathematical model.

	expression	remarks
variable	$P = \{P_1、P_2、\cdots P_i \cdots P_N\}$	Ship planning route point set
The objective function	Eq. (13)	Minimum safe potential energy path
Limiting conditions	Eq. (10)	Steer clear of obstacles
	Eq. (11)	The shipping route must meet the requirements of safe sailing water depth
	Eq. (12)	Inflection point of route should meet the ship's own turning limit

V. PATH IS GENERATED

A. PE-A* ALGORITHM

Potential energy can be used to digitally describe the environment and has the advantage of being precise. A* algorithm is A mature heuristic search algorithm, widely used in path planning, its outstanding advantage is that directional search can quickly calculate results and the results are accurate. The PE-A* algorithm is obtained by combining potential energy with A* algorithm. Based on the accurate description of obstacles by potential energy field, PE-A* algorithm can quickly plan the optimal route. PE-A* algorithm is mainly divided into three steps:

(1) environment construction
(2) environment search
(3) route generation

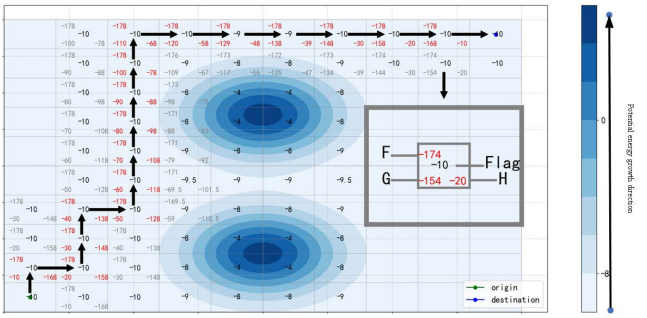

FIGURE 7. PE-A* algorithm operation diagram.

As shown in Fig. 7, the traction potential energy field between the origin and the destination is established and the obstacle is covered by the safety potential energy field. The value in the center of the grid represents the safety potential energy value $E_o\left(p\right)$ of grid P, open-set represents the nodes to be traversed and close-set represents the nodes that have been traversed. The heuristic function is shown in Ep. (14). Grid P: "Flag = E(P)" is the safe potential energy value of the grid is −10, "G = −154" is the safe potential energy sum of the path node from the starting point to the p point, "H = −20" is the minimum safe potential energy sum from the point to the destination, "F = −174" is the moving cost of the point. Search path from the starting point, to judge whether the current traction potential energy from the grid points to 0, when traction potential energy values are not zero to search, search direction for up, down, left, right, select search squares in the F value minimum grid as the next path nodes, repeat the process, until the grid search traction potential value of 0 to the finish, the arrow is the path.

$$\begin{cases} G = \int Flagd(close - set) \\ H = \dfrac{E\left(P\right) + E(end)}{2} * \sqrt[2]{\left(x_p + x_{end}\right)^2 + \left(y_p + y_{end}\right)^2} \end{cases} \tag{14}$$

B. DYNAMIC PROGRAMMING REGULATION

The minimum potential energy path nodes obtained by PE-A* algorithm can reflect the trend of the overall minimum potential energy path, but the overall path has too many nodes. According to the theorem "the sum of both sides of the triangle is greater than the third side," the path can be further simplified and the main path nodes can be selected. The mathematical model:

$$\left|\overrightarrow{a}\right| < \left|\overrightarrow{l_i}\right| + \left|\overrightarrow{l_{i+1}}\right| \tag{15}$$

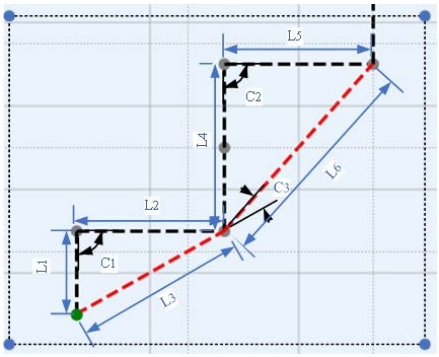

FIGURE 8. Schematic diagram of route node dynamic planning.

As shown in Fig. 8, sectionsL_1 and L_2 are optimized to L_3, and sections L_4 and L_5 are optimized to L_6. The steering angles C_1 of original sections L_1 and L_2 and C_2 of original sections L_4 and L_5 do not conform to the steering maneuvering limits of ships, while the steering angles C_3 of optimized sections L_3 and L_4 conform to the steering maneuvering limits of ships.

C. ROUTE PLANNING FRAMEWORK

As mentioned above, the route planning process based on PE-A* algorithm is as follows:

(1) Obtain relevant information: ship type information, longitude and latitude of origin and destination, elevation information of water area in route planning;
(2) According to the origin and destination, the traction potential energy field of the waterway planning area is established;
(3) The safety potential energy field of the ship is established according to the ship type information, and the safety potential energy threshold is determined according to the ship type information;
(4) By means of interpolating elevation data of navigational waters, the terrain elevation data with uniform scatter distribution is obtained, and the safety potential energy field of navigational waters is established;
(5) On the basis of traction potential energy field and safety potential energy field, PE-A* algorithm is used to calculate the path node of minimum safety potential energy path;
(6) The path nodes of minimum safe potential energy are dynamically programmed to obtain the global planned route;
(7) In the course of sailing in the global planning route, the ship needs to avoid collision locally when encountering new obstacles. The safety potential energy field of the new obstacles is established and superimposed to the original safety potential energy field to obtain the latest local safety potential energy field;
(8) Based on the traction potential energy field and the latest local safety potential energy field, the PE-A* algorithm is used in combination with the collision avoidance operation requirements of Ship Collision Avoidance Rules and the local obstacle avoidance path is obtained on the basis of the global planning path.

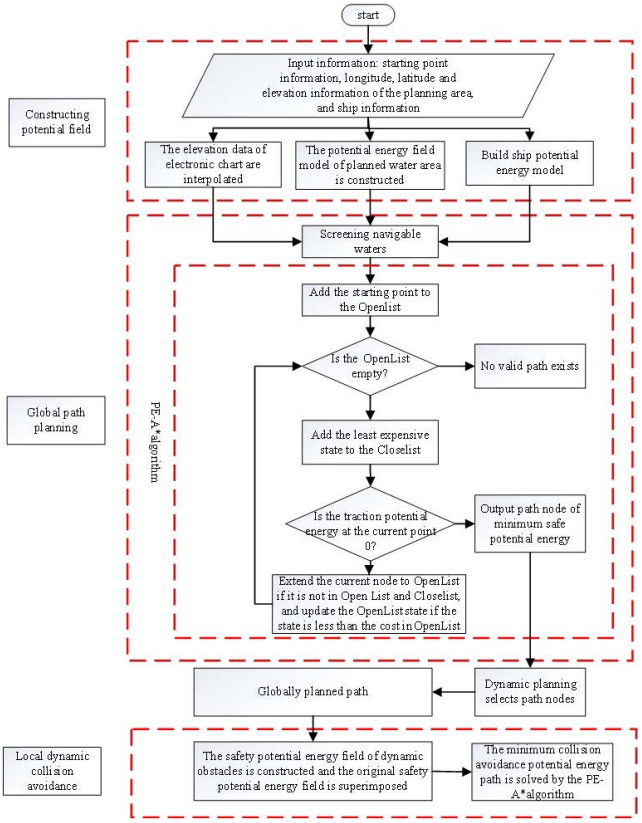

FIGURE 9. Flow chart of ship route planning based on PE-A * algorithm.

Fig. 9 shows the overall process. The calculations were performed on a computer with 4GB of ram and a 2.6ghz Intel Core I5 processor.

VI. CASE DESCRIPTION AND EXPERIMENTAL VERIFICATION

The main objectives of the experiment: (1) Establish a simulation experiment to describe the route planning process of PE-A * algorithm in detail; (2) Establish a comparative experiment to compare the results of A* algorithm and PE-A* algorithm, and verify the safety of PE-A* algorithm results by comparing the horizontal and vertical safety of the planned airline; (3) According to the actual electronic chart data, use

TABLE 3. Simulated ship information sheet.

The ship length L(m)	93
The ship width W(m)	15
The ship height H(m)	9
Ship turning restriction θ	5°~45°
Safe water depth D(m)	8

TABLE 4. Ship potential field parameter table.

X radius σ_{xt}(m)	$\sigma_{xt} = \frac{L}{2}$ =46.5
Y radius σ_{yt}(m)	$\sigma_{yt} = \frac{W}{2}$ =7.5
Potential energy at the center	$E(x, y) =$ 9
Safe potential energy threshold	E_{safe} =– D =– 8

PE-A* algorithm to calculate the route from Yang Kou Port S1 to Dafeng Port Dangerous Goods NO.4 anchorage, use PE-A* algorithm to plan the global route, add new obstacles, and use PE-A* algorithm again to plan the local obstacle avoidance route. The compatibility of PE-A* algorithm in global route planning and dynamic obstacle avoidance and the feasibility of route planning are verified.

The overall design of the experiment: The experiment consists of simulation experiment, contrast experiment and simulation experiment. Firstly, the specific planning process of PE-A* algorithm is described through simulation experiment. Then, the control variable method is used to compare the algorithm results in the comparison experiment, and the safety of the route planned by A* algorithm and PE-A* algorithm is discussed. Finally, combined with electronic chart data, PE-A* algorithm is used to plan the global route from Yang Kou port S1 to Dafeng Port dangerous goods NO.4 anchorage and dynamic obstacles are designed to plan local collision avoidance paths.

A. SIMULATION EXPERIMENT

In this simulation experiment, the navigation area of {40000m × 40000m} is established, origin, destination, 11 static obstacles and 1 dynamic obstacle are set within the area, PE-A* algorithm is used to realize global route planning and local collision avoidance.

1) CONSTRUCT OUR SHIP POTENTIAL ENERGY FIELD

Suppose the ship information of the simulation experiment is shown in the Table 3, the ship potential energy field is established according to the ship information, and the potential energy parameters are shown in the Table 4:

2) CONSTRUCT TRACTION POTENTIAL ENERGY FIELD

As shown in the Table 5, the selected area of the simulation experiment is {40000m × 40000m}, which is the origin (0,0) and the destination (40000,40000) of the simulation experiment. The larger the distance from the destination, the greater the traction potential energy of the ship. On the contrary, the smaller the traction potential energy of the ship.

TABLE 5. Table of traction potential field parameters.

Point P	(x_p, x_p)
origin	$(x_{origin}, y_{origin}) = (0,0)$
destination	$(x_{destination}, y_{destination}) = (40000,40000)$

TABLE 6. Table of safe potential energy parameters of obstacles.

Obstacle number	Potential energy at the center	Center point coordinates	X radius σ_{xt}(m)	Y radius σ_{yt}(m)
1	10	(5000, 30000)	2500	2500
2	20	(10000,6000)	1500	1000
3	2	(10000,17000)	10000	10500
4	25	(7000,8000)	2700	2900
5	24	(15000,20000)	2300	2400
6	39	(36000,19000)	2800	2300
7	25	(20000,20000)	2500	2000
8	-25	(20000,10000)	30000	30000
9	15	(30000,31000)	2500	3000
10	25	(25000,9000)	2200	1900
11	37	(30000,38000)	2600	2200

3) CONSTRUCT A SAFE POTENTIAL ENERGY FIELD

Obstacles have a hindering effect on ship navigation. This simulation experiment designed 11 to simulate obstacles and establish the safety potential energy field of obstacles. At different positions of the ship's safe potential energy field, the safe potential energy value of this point reflects the sailing risk of the ship at this point, as shown in FIG. 9: The darker the color is, the higher the safe potential energy value of this point is, and the greater the sailing risk is. On the contrary, the lower, the less navigation risk. The obstacle information selected in this simulation experiment is shown the Table 6:

4) DIVISION OF NAVIGABLE WATERS

According to my ship model of potential energy available, ship safety potential value $E_{safe} = -8$, combined with the safety potential energy field, the navigable waters of simulation with navigation area are differentiated, as shown in Fig. 10: red scatter distribution areas are safety potential energy greater than the threshold, the potential energy is not sailing area, ship can collide in the area. Otherwise, ship can safely navigate in the area.

5) GLOBAL ROUTE PLANNING

Under the joint influence of traction potential energy field and safety potential energy field, PE-A * algorithm is used to search with step size of 2000m, the minimum safety potential energy path node is obtained. Based on the route node of the minimum safe potential energy and combined with the ship turning restriction, dynamic planning is carried out to select the main route nodes in the global planning. The global planning route nodes are shown in the Table 7, the global planning route nodes are shown in green route in Fig. 10:

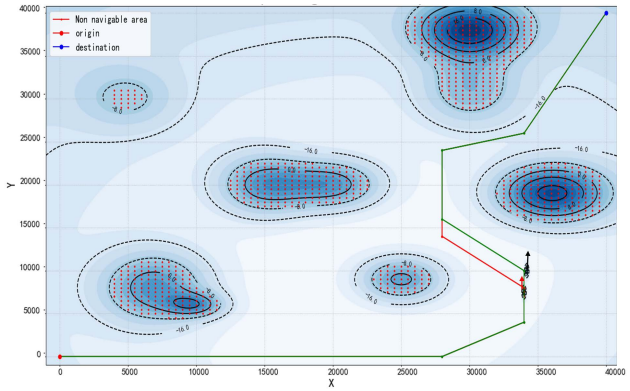

FIGURE 10. Schematic diagram of simulated experimental route planning.

TABLE 7. Plan route nodes globally.

Main path node	[[40000, 40000], [34000, 26000], [28000, 24000], [28000, 14000], [34000, 8000], [34000, 2000], [26000, 0], [0, 0]]

TABLE 8. Local dynamic collision avoidance node.

Main path node	[[40000, 40000], [34000, 26000], [28000, 24000], [28000, 16000], [34000, 10000], [34000, 2000], [26000, 0], [0, 0]]

6) LOCAL DYNAMIC COLLISION AVOIDANCE

Set the dynamic obstacle as the ship of the same type as our ship. When our ship sailing along the global path planning to this position, the two ships formed an encounter situation. Black arrow shows this ship's sailing direction, red arrow shows ship sailing direction for me. In order to overtake the vessel, our ship shall take collision avoidance action according to the regulations of collision avoidance. Firstly, according to the relevant information of the new obstacle, the safety potential energy field of the dynamic obstacle is established, which is superimposed with the original safety potential energy field to obtain the updated hindrance potential energy field. Then, the pe-A * algorithm is used to search the updated safe potential energy field with a step length of 50 m, and the local minimum safe potential energy path node is obtained. Finally, the local obstacle avoidance route is obtained by dynamic programming based on the local minimum potential energy path node. Local obstacle avoidance route nodes are shown in the Table 8, as shown in Fig. 10: The red route is the local obstacle avoidance route.

B. COMPARATIVE EXPERIMENTS

The above simulation experiment environment is still selected, and the control variable method is used to compare the safety of the route planned by A* algorithm and PE-A* algorithm. In the comparison experiment, the difference between A* algorithm and PE-A* algorithm:

(1) Environment construction: A* algorithm often adopts raster map, "Flag = 1" means that there are obstacles in this grid, which is unnavigable point, "Flag = 0" means that there are no obstacles in this grid, which is navigable point; PE-A* algorithm uses potential energy field to describe obstacles in detail "Flag = E", where $E > E_{safe}$ is the unnavigable point, and vice versa.

(2) Heuristic function: A* algorithm heuristic function is:

$$\begin{cases} G = \int Flag\ d\ (close - set) \\ H = \sqrt[2]{(x_p + x_{end})^2 + (y_p + y_{end})^2} \end{cases} \tag{16}$$

PE-A* algorithm heuristic function is:

$$\begin{cases} G = \int \text{Flag}\ d\ (\text{close} - \text{set}) \\ H = \dfrac{E\ (P) + E(end)}{2} * \sqrt[2]{(x_p + x_{end})^2 + (y_p + y_{end})^2} \end{cases} \tag{17}$$

TABLE 9. Route length table.

	A* algorithm for route planning	PE-A* algorithm for route planning
Planned route length	63830.6	80513.5

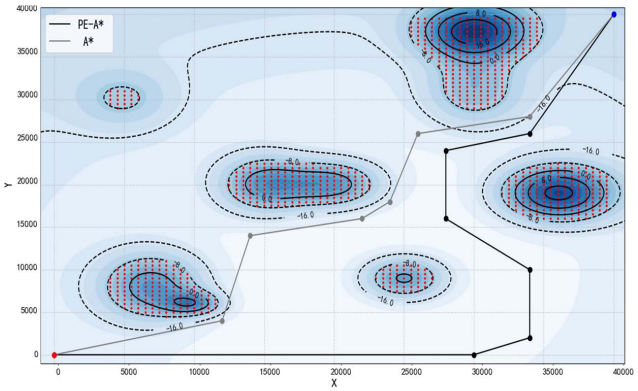

FIGURE 11. Schematic diagram of comparing experimental route planning.

As shown in Fig. 11, gray routes are planned by A* algorithm, black routes are planned by PE-A* algorithm. The length of routes is shown in the Table 9:

The safety evaluation basis of shipping route is as follows: from the safety perspective of planning shipping route, it is required not only to avoid obstacles in horizontal dimension, but also to meet the longitudinal water depth of the ship's draft. The farther the distance between the planned route and the unnavigable point in the horizontal dimension, the higher the horizontal safety; The deeper the depth of the planned waypoint in the longitudinal dimension, the higher the longitudinal safety.

1) HORIZONTAL SECURITY

Horizontal safety: In the horizontal dimension, the smaller the distance between the planned path and the nearest non-navigable area, the higher the risk of collision and the lower

TABLE 10. Horizontal safety gauge.

Distance between level and unnavigable point (m)	A* algorithm	Segment of A* algorithm	PE-A* algorithm	Segment of PE-A* algorithm
<100	1225.76	1.92%	0	0%
<200	12532.6	19.63%	0	0%
<300	37152.0	58.20%	0	0%
<400	46968.7	73.58%	1581.1	1.96%
<500	56633,7	88.73%	25128.7	31.21%
<600	60352.11	94.55%	36466.3	45.29%
<700	63830.6	100%	42417.7	52.68%

the horizontal safety; on the contrary, horizontal security is higher.

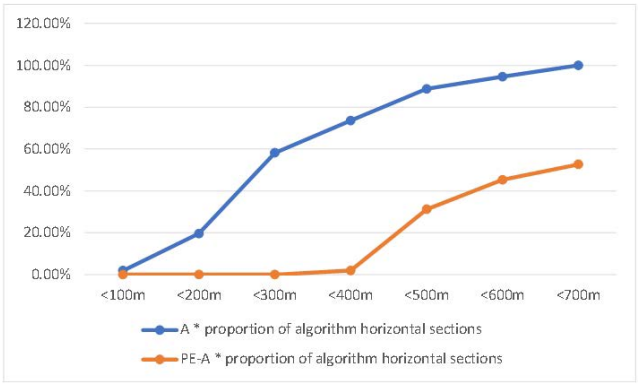

FIGURE 12. Compare the horizontal safety line chart of the experimental route.

As can be seen from the Table 10 and Fig. 12, the proportion of planned route of A* algorithm increases rapidly with the increase of distance from unnavigable points, while that of PE-A* algorithm increases almost to zero before <400m Segment growth, and then presents A rapid growth trend. The segment with less than 400m distance between the route planned by PE-A* algorithm and unnavigable points accounts for only 1.96%, while the segment of A* algorithm accounts for as much as 73.58%. In the <700m segment, the route planned by PE-A* algorithm accounts for 52.68%, while the segment planned by A* algorithm has reached 100%. In the horizontal dimension, the path obtained by PE-A* algorithm is better than that obtained by A* algorithm. The path is far from the unnavigable area, the ship has a larger operating space in case of emergency. The horizontal safety degree is as follows: PE-A* algorithm ≫A* algorithm.

2) LONGITUDINAL SAFETY

Longitudinal safety: in longitudinal dimension, the smaller the longitudinal water depth of the planned path, the higher the risk of stranding or bottom collision, the lower the longitudinal safety; on the contrary, longitudinal safety is higher.

It can be seen from the Table 11 and Fig. 13 that the proportion of sections with water depth <12m is 0%

TABLE 11. Longitudinal safety gauge.

Vertical depth (m)	A* algorithm	Segment of A* algorithm	PE-A* algorithm	Segment of PE-A* algorithm
<12	0	0%	0	0%
<14	6355.73	9.96%	4123.10	5.12%
<16	20719.67	32.46%	9047.09	11.29%
<18	28573.2	44.76%	17319.60	21.51%
<20	44679.84	69.98%	20828.86	25.87%

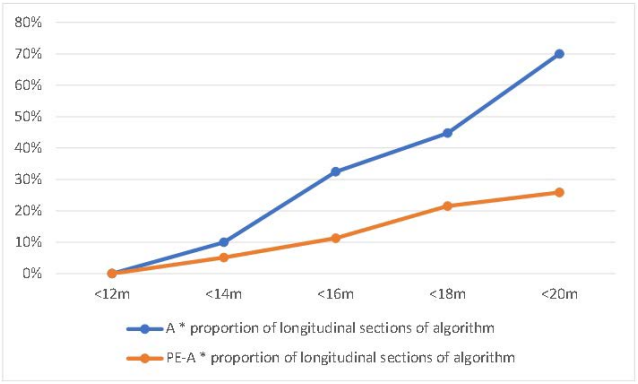

FIGURE 13. Compare the longitudinal safety line chart of the experimental route.

according to PE-A* algorithm and A* algorithm. With the increase of water depth, the proportion of road length of PE-A* algorithm is less than that of A* algorithm. PE-A* algorithm is less than A* algorithm in the trend of water depth expansion. In the water depth <20m A* algorithm ≫PE-A* algorithm. Therefore, in the planning route of PE-A* algorithm, the risk of ship grounding and other dangers is less, and the longitudinal safety degree is: PE-A* algorithm >A* algorithm.

Different from vehicles and airplanes, ships belong to 2.5-dimensional means of transportation, the influence of horizontal navigation space and underwater navigation space on ships needs to be considered simultaneously. Moreover, the ship's operation is delayed, requiring a larger safety space. A* algorithm only considers the distance, and only considers the sailing distance without considering the characteristics of the ship's navigation. For the ship, the planned route is often not feasible. PE-A* algorithm of planning path in space security greatly improves the feasibility.

C. SIMULATION EXPERMENT

Ships navigate in large open waters such as the Pacific Ocean, the great circle route can meet the needs of ocean route planning. Moreover, due to the large scope of international ocean navigation, the visualization effect of the experimental results of global route planning and local dynamic obstacle avoidance is poor. Therefore, this experiment selects the medium range area as the experimental object to verify the practical feasibility of the algorithm and achieve good visualization effect at the same time.

TABLE 12. Ship potential field parameter table.

X radius σ_{xt}(m)	$\sigma_{xt} = \frac{L}{2} = 45$
Y radius σ_{yt}(m)	$\sigma_{yt} = \frac{W}{2} = 6$
Potential energy at the center	$E(x, y) = 8$
Safe potential energy threshold	$E_{safe} = -\mathrm{D} = -7$

The range of longitude [120.6, 122.4] and latitude [32.2, 33.9] is selected as the range of route planning. The origin is Yang Kou Port S1 with coordinates [121.572,32.591] and the destination is Dafeng Port Dangerous Goods NO.4 anchorage with coordinates [120.906,33.203]. Due to the actual water depth limitation of the region, the chemical vessel was used as the experimental vessel.

Firstly, the ship potential energy field model is established, as shown in the Table 12. Then, the traction potential energy field is established according to the origin and destination, based on the electronic chart data, the mean interpolation processing is carried out to obtain the evenly distributed chart data, and the safety potential energy field of the waterway planning area is established. The traction potential energy field is shown in the Fig.14, the safe potential energy field is shown in the Fig. 15:

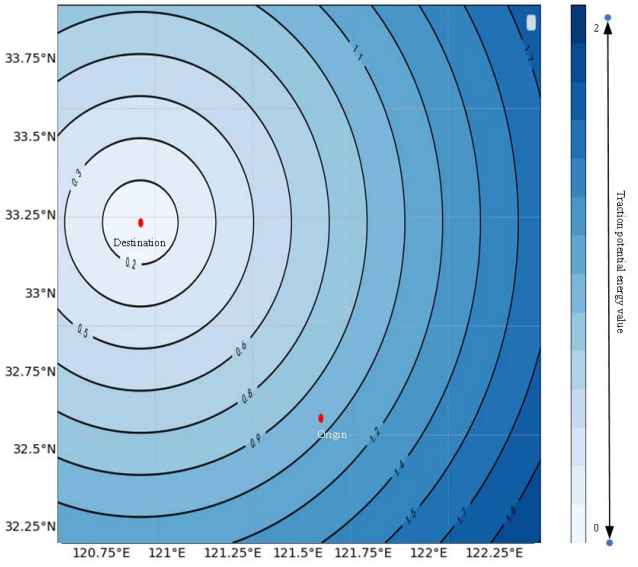

FIGURE 14. Schematic diagram of traction potential energy field in simulation experiment.

A 100 × 100 grid was used to cover the planned water area, the PE-A* algorithm was used to search the path node of the minimum potential energy, and the main path node of the global path was extracted by dynamic programming. The global planning route is shown in Fig. 16 and Fig. 17. global path is integrated into the safety potential energy field and the actual electronic chart. It can be observed in the electronic chart that the route of box 1 and box 2 is closer to the obstacle than other sections of the global route. As are

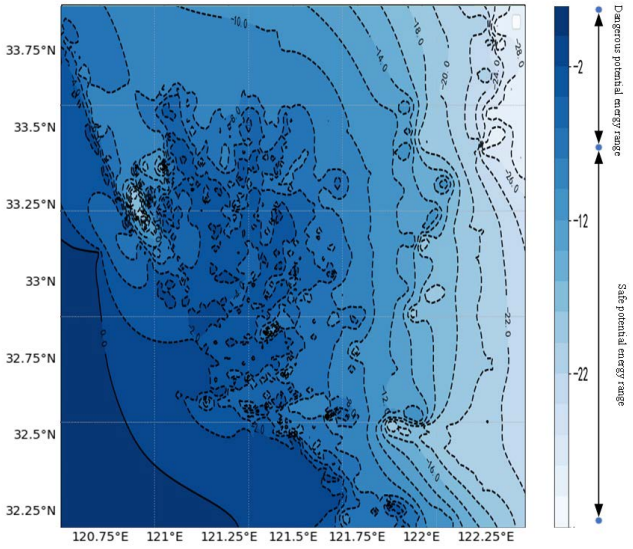

FIGURE 15. Schematic diagram of safety potential energy field in simulation experiment.

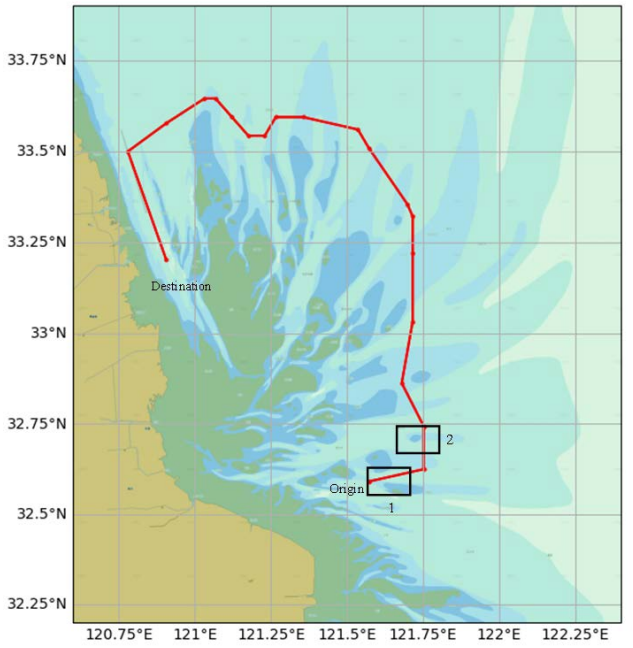

FIGURE 16. Simulation experiment: global planning course chart based on electronic chart.

TABLE 13. Global plan course point list.

Main path node	[[120.906, 33.203], [120.78, 33.500], [120.906, 33.577], [121.032, 33.645], [121.068, 33.645], [121.122, 33.594], [121.176, 33.543], [121.230, 33.543], [121.266, 33.594], [121.356, 33.594], [121.536, 33.560], [121.572, 33.509], [121.698, 33.356], [121.716, 33.322], [121.716, 33.220], [121.716, 33.033], [121.680, 32.863], [121.752, 32.744], [121.752, 32.625], [121.572, 32.591]]

shown in Fig. 18 and Fig. 19, the area within box 1 and box 2 can be enlarged and observed, and the water depth of the route

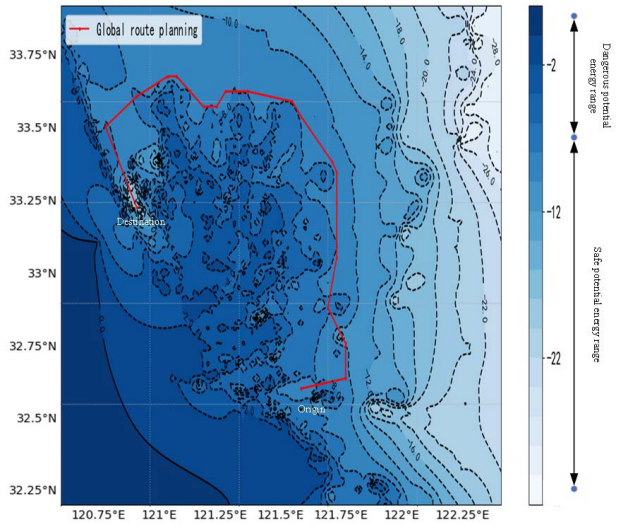

FIGURE 17. Simulation experiment: global planning route map based on safety potential energy field.

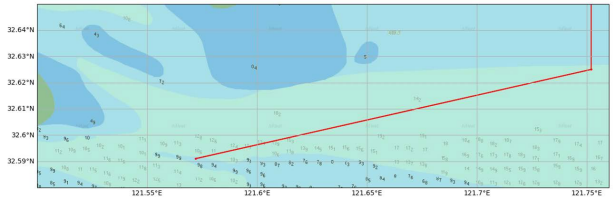

FIGURE 18. Simulation experiment: planning course chart based on box 1 electronic chart.

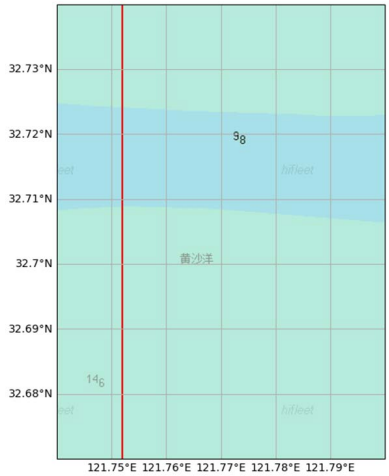

FIGURE 19. Simulation experiment: planning course chart based on box 2 electronic chart.

of box 1 ranges from 10.6m to 15.3m. In box 2, the water depth range is 9.8m to 14.6m. In summary, the whole section of the planned route meets the navigation requirements of ships. The global route points are shown in the Table 13.

When sailing along the global planning path, our ship encountered a temporary navigation ban in the area as shown in Fig. 20, which required emergency obstacle avoidance. The gray area is the area of ship collision accident, which intersects with the global planning route of our ship. The

TABLE 14. Table of safe potential energy parameters of dynamic obstacles.

Obstacle avoidance	Potential energy at the center	Center-point coordinates	X radius σ_{xt} (km)	Y radius σ_{yt} (km)
military practice area	15.0	[121.3, 33.59]	7.0	7.0

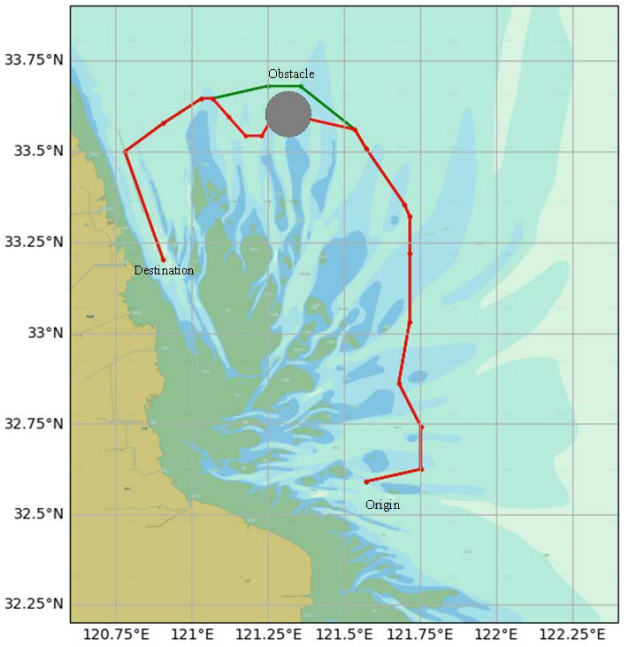

FIGURE 20. Simulation experiment: local dynamic collision avoidance course map based on electronic chart.

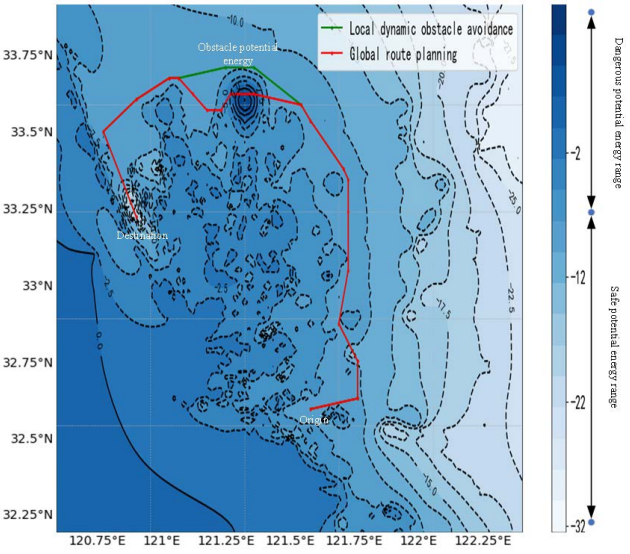

FIGURE 21. Simulation experiment: Local dynamic collision avoidance route map based on safety potential energy field.

safety potential energy parameters of this area are shown in table 14. The safety potential energy field was established and superimposed to the original safety potential energy field to obtain the latest safety potential energy field as shown in

TABLE 15. List of local collision avoidance course points.

Main path node	[[120.906, 33.203], [120.780, 33.500], [120.906, 33.577], [121.032, 33.645], [121.068, 33.645], [121.248, 33.679], [121.356, 33.679], [121.536, 33.560], [121.572, 33.509], [121.698, 33.356], [121.716, 33.322], [121.716, 33.220], [121.716, 33.033], [121.680, 32.863], [121.752, 32.744], [121.752, 32.625], [121.572, 32.591]]

Fig. 21. The PE-A* algorithm was used to solve the local obstacle avoidance route. As shown in Fig. 20 and Fig. 21, the reality of local collision avoidance routes under the safety potential energy field and electronic chart, the green route is the global planning path, and the red route is the obstacle avoidance path. Local obstacle avoidance route nodes are shown in the Table 15:

VII. CONCLUSION

This study mainly focuses on explanation. A* algorithm is a mature heuristic search algorithm and potential energy field can describe the characteristics of obstacles well. By combining the advantages of A* algorithm and potential energy, PE-A* algorithm can take into account both global route planning and local dynamic collision avoidance. PE-A* algorithm takes into account both global route planning and local dynamic collision avoidance. Experimental results show that the route planned by PE-A* algorithm has good effect in both horizontal dimension and vertical dimension, can greatly reduce the risk of ship collision and grounding. The mathematical model in this study can adjust the value basis of potential energy according to the needs of the shipping company, plan the optimal route under different objectives. Model in this study considers fewer constraints, which can be adjusted according to the actual situation, such as: bridge constraints of inland rivers, cyclone in the ocean, wind, current, wave, etc.

A. ABOUT MATHEMATICAL MODELS

The purpose is to find the optimal path of ship navigation, there are many factors for the optimal path test rate, such as: path length, safety, ship fuel consumption, loss and other factors. Theoretically, considering more factors, the planned ship path will be more optimized and reliable, which is convenient for shipping companies to carry out more accurate voyage cost estimation. This study mainly explains the PE-A* algorithm and its solving process by planning the safest path. In the future research, we can further find the safe navigation path from the perspective of wind, current, wave and potential energy. This study only considers a pair of simple objects, navigation safety and path length, to provide a simple understanding of ship path optimization.

B. ENVIRONMENT DESCRIPTION

In this study, by introducing the concept of potential energy field, obstacles and ships are covered by potential energy field. Gaussian model is mainly used for mathematical description in function model. But the contour of obstacles is complex and cannot be simply described by a single model in practice. Therefore, the next step is to find a more accurate function model to reproduce obstacles, so as to make the optimization model more fit the reality and further improve the feasibility of the path.

C. ABOUT ALGORITHMS

A* algorithm is a mature algorithm in heuristic search algorithm, algorithm has fast convergence, can get results in a short time. Potential energy can accurately describe obstacles. Combining A* algorithm with potential energy, PE-A* algorithm can not only ensure the accurate description of obstacles, but also ensure the timeliness of the algorithm. It can be concluded from the experiment, that the route planned by the PE-A * algorithm is more optimized. By establishing potential energy field, it can accurately describe the navigation waters digitally. When a new obstacle appears in the navigation waters, the potential energy field of the new obstacle is superposed on the original potential energy field, so that the PE-A* algorithm can take into account both global route planning and local dynamic collision avoidance. PE-A* algorithm can improve the navigation safety of ships in both horizontal and vertical dimensions, which greatly improves the practicability of route planning.

REFERENCES

[1] C. Cheng, Q. Sha, B. He, and G. Li, "Path planning and obstacle avoidance for AUV: A review," *Ocean Eng.*, vol. 235, no. 1, pp. 34–39, Sep. 2021, doi: 10.1016/j.oceaneng.2021.109355.

[2] D. Zhang, Y. Zhang, and C. Zhang, "Data mining approach for automatic ship-route design for coastal seas using AIS trajectory clustering analysis," *Ocean Eng.*, vol. 236, pp. 1–16, Jul. 2021, doi: 10.1016/j.oceaneng.2021.109535.

[3] L. Bui-Duy and N. Vu-Thi-Minh, "Utilization of a deep learning-based fuel consumption model in choosing a liner shipping route for container ships in Asia," *Asian J. Shipping Logistics*, vol. 37, no. 1, pp. 1–11, Mar. 2021, doi: 10.1016/j.ajsl.2020.04.003.

[4] Y. Wen, Z. Sui, C. Zhou, C. Xiao, Q. Chen, D. Han, and Y. Zhang, "Automatic ship route design between two ports: A data-driven method," *Appl. Ocean Res.*, vol. 96, pp. 1–12, Dec. 2019, doi: 10.1016/j.apor.2019.102049.

[5] J. Szlapczynska and R. Szlapczynski, "Preference-based evolutionary multi-objective optimization in ship weather routing," *Appl. Soft Comput.*, vol. 84, Nov. 2019, Art. no. 105742, doi: 10.1016/j.asoc.2019.105742.

[6] T.-N. Chuang, C.-T. Lin, J.-Y. Kung, and M.-D. Lin, "Planning the route of container ships: A fuzzy genetic approach," *Expert Syst. Appl.*, vol. 37, no. 4, pp. 2948–2956, Apr. 2010, doi: 10.1016/j.eswa.2009.09.040.

[7] C. Liang, X. Zhang, and X. Han, "Route planning and track keeping control for ships based on the leader-vertex ant colony and nonlinear feedback algorithms," *Appl. Ocean Res.*, vol. 101, pp. 1–8, Jun. 2020, doi: 10.1016/j.apor.2020.102239.

[8] X. Lan, X. Lv, W. Liu, Y. He, and X. Zhang, "Research on robot global path planning based on improved A-star ant colony algorithm," in *Proc. IEEE 5th Adv. Inf. Technol., Electron. Autom. Control Conf. (IAEAC)*, Mar. 2021, pp. 613–617, doi: 10.1109/IAEAC50856.2021.9391099.

[9] M. Li and H. Zhang, "AUV 3D path planning based on A* algorithm," in *Proc. Chin. Autom. Congr. (CAC)*, May 2021, pp. 11–16, doi: 10.1109/CAC51589.2020.9327873.

[10] Q. Han, X. Yang, H. Song, S. Sui, H. Zhang, and Z. Yang, "Whale optimization algorithm for ship path optimization in large-scale complex marine environment," *IEEE Access*, vol. 8, pp. 57168–57179, 2020, doi: 10.1109/access.2020.2982617.

[11] J. Wang and Z. Chen, "A novel hybrid map based global path planning method," in *Proc. 3rd Asia–Pacific Conf. Intell. Robot Syst.*, 2018, pp. 66–70, doi: 10.1109/acirs.2018.8467225.
[12] W. Xie, X. Fang, and S. Wu, "2.5D navigation graph and improved a-star algorithm for path planning in ship inside virtual environment," in *Proc. Prognostics Health Manage. Conf.*, Jul. 2020, pp. 295–299, doi: 10.1109/PHM-Besancon49106.2020.00057.
[13] W. Zhang, C. Yan, H. Lyu, P. Wang, Z. Xue, Z. Li, and B. Xiao, "COLREGS-based path planning for ships at sea using velocity obstacles," *IEEE Access*, vol. 9, pp. 32613–32626, 2021, doi: 10.1109/ACCESS.2021.3060150.
[14] T. Liu, Z. Huang, W. Tang, and Z. Wang, "Research of automatic collision avoidance based on ship maneuvering," in *Proc. Int. Conf. Ind. Inform.*, Dec. 2016, pp. 232–235, doi: 10.1109/ICIICII.2016.0063.
[15] L. Xie, S. Xue, J. Zhang, M. Zhang, W. Tian, and S. Haugen, "A path planning approach based on multi-direction A* algorithm for ships navigating within wind farm waters," *Ocean Eng.*, vol. 184, pp. 311–322, Jul. 2019, doi: 10.1016/j.oceaneng.2019.04.055.
[16] B. Li, R. Chiong, and L. Gong, "Search-evasion path planning for submarines using the artificial bee colony algorithm," *IEEE Congr. Evol. Comput.*, vol. 6, no. 11, pp. 528–535, Jul. 2014, doi: 10.1109/cec.2014.6900224.
[17] L. Su, X.-J. Qin, Z.-L. Liu, and Z. Zhang, "Intelligent collision avoidance decision for single ship considering ship maneuverability," in *Proc. 9th Int. Conf. Inf. Sci. Technol. (ICIST)*, Aug. 2019, pp. 164–168, doi: 10.1109/icist.2019.8836732.
[18] H. Liu, R. Deng, and L. Zhang, "The application research for ship collision avoidance with hybrid optimization algorithm," in *Proc. IEEE Int. Conf. Inf. Autom. (ICIA)*, Aug. 2016, pp. 760–767, doi: 10.1109/icinfa.2016.7831921.
[19] W. Xu, J. Yin, J. Hu, and K. Li, "Ship automatic collision avoidance by altering course based on ship dynamic domain," in *Proc. IEEE TrustCom*, Aug. 2016, pp. 2024–2030, doi: 10.1109/TrustCom.2016.0309.
[20] J. Yu, Z. Liu, R. Bu, X. Gao, and W. Li, "A novel fast decision-making method for ship's course altering for collision avoidance," in *Proc. Chin. Autom. Congr. (CAC)*, 2020, pp. 2203–2207, doi: 10.1109/cac51589.2020.9327213.
[21] B. Shi, Y. Su, C. Wang, L. Wan, and Y. Qi, "Recovery path planning algorithm based on Dubins curve for autonomous underwater vehicle," in *Proc. IEEE 8th Int. Conf. Underwater Syst. Technol., Theory Appl. (USYS)*, Dec. 2018, pp. 1–5, doi: 10.1109/USYS.2018.8778859.
[22] H. Jincan and F. Maoyan, "Based on ECDIS and AIS ship collision avoidance warning system research," in *Proc. 8th Int. Conf. Intell. Comput. Technol. Autom. (ICICTA)*, Jun. 2015, pp. 242–245, doi: 10.1109/icicta.2015.69.
[23] Y. Chen and T. Li, "Collision avoidance of unmanned ships based on artificial potential field," in *Proc. Chin. Autom. Congr. (CAC)*, Jan. 2018, pp. 4437–4440, doi: 10.1109/CAC.2017.8243561.
[24] H. Namgung and J.-S. Kim, "Collision risk inference system for maritime autonomous surface ships using COLREGs rules compliant collision avoidance," *IEEE Access*, vol. 9, pp. 7823–7835, 2021, doi: 10.1109/access.2021.3049238.
[25] S. Wang, Y. Zhang, and L. Li, "A collision avoidance decision-making system for autonomous ship based on modified velocity obstacle method," *Ocean Eng.*, vol. 4, pp. 1–21, Aug. 2020, doi: 10.1016/j.oceaneng.2020.107910.
[26] X. Zhang, H. Wang, H. Lv, and Q. Li, "UUV dynamic path planning and trap escape strategies in unknown environment," in *Proc. 35th Chin. Control Conf. (CCC)*, Jul. 2016, pp. 6988–6992, doi: 10.1109/chicc.2016.7554458.
[27] Y. Tian, L. Huang, Y. Xiong, and S. Li, "On the velocity obstacle based automatic collision avoidance with multiple target ships at sea," in *Proc. Int. Conf. Transp. Inf. Saf. (ICTIS)*, Jun. 2015, pp. 468–472, doi: 10.1109/ICTIS.2015.7232097.
[28] Q. Wang, M. Zhong, G. Shi, J. Zhao, and C. Bai, "Route planning and tracking for ships based on the ECDIS platform," *IEEE Access*, vol. 9, pp. 71754–71762, 2021, doi: 10.1109/ACCESS.2021.3078899.
[29] L. Wang, Z. Zhang, Q. Zhu, and S. Ma, "Ship route planning based on double-cycling genetic algorithm considering ship maneuverability constraint," *IEEE Access*, vol. 8, pp. 190746–190759, 2010, doi: 10.1109/access.2020.3031739.
[30] D. Ni and H. Wang, "A unified perspective on traffic flow theory. Part III: Validation and benchmarking," *Appl. Math. Sci.*, vol. 7, no. 40, 2013, pp. 1965–1982.
[31] D. Ni, "A unified perspective on traffic flow theory. Part II: The unified diagram," *Appl. Math. Sci.*, vol. 7, no. 40, 2013, pp. 1947–1963.
[32] D. Ni, "A unified perspective on traffic flow theory Part I: The field theory," *Appl. Math. Sci.*, vol. 7, no. 39, pp. 1929–1946. 2013.

YIHUA LIU was born in Hunan, China, in 1980. He received the B.S. degree in marine navigation, the M.Sc. degree in vehicle operation, and the Ph.D. degree in vehicle operation engineering from Shanghai Maritime University, in 2002, 2004, and 2020, respectively. He is currently a Doctoral Supervisor and an Associate Professor with the Merchant Marine College, Shanghai Maritime University. His research interests include maritime intelligent transportation and traffic information engineering and control.

TING WANG was born in Anhui, China, in 1997. She is currently pursuing the master's degree in vehicle operation engineering with the Merchant Marine College, Shanghai Maritime University. Her research interests include maritime traffic engineering and global meteorological navigation.

HONGZHI XU was born in Shandong, China, in 1972. He received the M.Sc. degree major in naval architecture and ocean engineering from the Jiangsu University of Science and Technology. He is a Senior Engineer and a Principal Certified Marine Surveyor, he has been engaged in technology fields, such as the research and exploration, design and manufacture, inspection and utilization of vessels, and offshore structures. He has hosted three scientific research items at ministerial/provincial level, such as "Research on Key Technology of Polar Tankers," published 13 pieces of academic papers, held seven patents, and jointly trained two master's.